# Functional genomics in primary T cells and monocytes identifies mechanisms by which genetic susceptibility loci influence systemic sclerosis risk

David González-Serna[1,$,*], Chenfu Shi[2,$], Martin Kerick[1], Jenny Hankinson[3], James Ding[2], Amanda McGovern[2], Mauro Tutino[3], Norberto Ortego-Centeno[4], José Luis Callejas[4], Javier Martin[1,§] & Gisela Orozco[2,5,§,*]

[1]Institute of Parasitology and Biomedicine López-Neyra, Consejo Superior de Investigaciones Científicas (IPBLN-CSIC), Granada, Spain.
[2]Centre for Genetics and Genomics Versus Arthritis, Division of Musculoskeletal and Dermatological Sciences, School of Biological Sciences, Faculty of Biology, Medicine and Health, The University of Manchester, Manchester, UK.
[3]Division of Infection, Immunity & Respiratory Medicine, School of Biological Sciences, Faculty of Biology, Medicine and Health, The University of Manchester, Manchester, UK.
[4]Department of Internal medicine, Hospital Universitario San Cecilio, Institute for Biosanitary Research of Granada (ibs.GRANADA), Granada, Spain.
[5]NIHR Manchester Biomedical Research Centre, Manchester University NHS Foundation Trust, Manchester Academic Health Science Centre, Manchester, UK.
[$]Joint first authors.
[§]Joint senior authors.

*Correspondence to David González-Serna (email: sna.david@ipb.csic.es) and Gisela Orozco (Gisela.Orozco@manchester.ac.uk)

**Funding:** This work was supported by the Spanish Ministry of Science and Innovation (grants RTI2018101332-B-100 and SAF2015-66761-P), the Cooperative Research Thematic Network (RETICS) programme (RD16/0012/0013) (RIER) from Instituto de Salud Carlos III (ISCIII, Spanish Ministry of Economy, Industry and Competitiveness), the Wellcome Trust (award references 207491/Z/17/Z and 215207/Z/19/Z), Versus Arthritis (award reference 21754), and the NIHR Manchester Biomedical Research Centre.

## ABSTRACT

**Objectives.** Systemic sclerosis (SSc) is a complex autoimmune disease with a strong genetic component. However, most of the causal genes and variants are still unknown. The challenge in the post-GWAS era is to use functional genomics to translate genetic findings into patients' benefit, particularly in disease-relevant cell types.

**Methods.** Promoter capture Hi-C (pCHi-C) and RNA sequencing experiments were performed in a total of 30 samples corresponding to $CD4^+$ T cells and $CD14^+$ monocytes (15 samples each) from SSc patients and healthy controls to link SSc-associated variants with their target genes, followed by differential expression and differential interaction analyses between both cell types. We also aimed to identify potential drugs that could be repurposed for its use in SSc.

**Results.** We linked SSc-associated loci to 39 new potential target genes, confirming 7 previously assigned genes. We highlight novel causal genes, such as *CXCR5* as the most probable candidate gene for the *DDX6* locus. Some SSc confirmed genes such as *IRF8, STAT4*, or *CD247* interestingly showed cell type specific interactions. We also identified 15 potential drug targets already in use in other similar immune-mediated diseases that could be repurposed for SSc treatment. Furthermore, we observed that interactions are directly related with the expression of important genes implicated in cell type specific pathways.

**Conclusions.** Our study reveals potential causal genes for SSc-associated loci, some of them acting in a cell type specific manner, suggesting novel biological mechanisms that may mediate SSc pathogenesis.

# INTRODUCTION

Systemic sclerosis (SSc) is a complex chronic immune-mediated disease that affects the connective tissue, characterized by an immune imbalance, vascular alterations, and an excessive collagen deposition leading to fibrosis (1). Several lines of evidence implicate T cells and monocytes/macrophages as important cell types in SSc pathogenesis (2,3). In this regard, modifications in the proportions of $CD4^+$ T cell subpopulations, and their functional alterations may contribute to the vascular dysregulation and fibrosis observed in the disease (4,5). On the other hand, circulating monocytes/macrophages with a profibrotic phenotype are increased in blood from SSc patients (6,7), and changes in human monocyte-derived macrophages transcriptome are related to SSc genetic variants (8).

SSc presents a complex genetic component and its etiology is poorly understood. Large-scale genetic studies have so far identified 27 independent signals associated with susceptibility to SSc (9,10). Interestingly, many of the different genes assigned to SSc GWAS loci are related to T cell activation and macrophages regulation pathways (11,12), and are shared among immune-mediated diseases, which may be of interest in the drug repositioning of rare diseases like SSc, where there are no specific available treatments (13). However, the majority of single nucleotide polymorphisms (SNPs) associated with SSc map to non-coding regions of the genome that are enriched in enhancer elements, which are cell-type specific (14,15). These regulatory elements can interact with genes often located hundreds of kilobases away, bypassing nearby genes in many cases (16).

Thus, the current challenge remains in linking disease-associated regions with the genes that they have an effect on, and the specific cell types involved, in order to point to the mechanisms of regulation and the biological pathways implicated in genetically susceptible patients (17). In this regard, many three-dimensional genome architecture techniques have emerged, such as chromosome conformation capture (3C) (18,19). The most powerful technique developed to date, Hi-C (high throughput chromosome conformation capture) allows the genome-wide identification of chromosomal interactions within a cell population (20). A more recent technique, capture Hi-C (CHi-C) allows to specifically enrich chromosomal regions of interest, such as disease risk loci (region CHi-C) or promoters (promoter CHi-C, pCHi-C) from Hi-C libraries in a cost-effective way (21). This technique has been successfully applied in different cell types to link enhancers and non-coding disease variants to potential target genes (22). Previously, we successfully applied CHi-C to identify disease causal genes and potential drugs for repositioning in autoimmune diseases using cell lines (23,24). Since the regulation of gene expression is highly context specific, it is essential to apply these technologies to primary cells isolated from patients.

In this study, we apply pCHi-C technology in the most relevant cell types in SSc pathogenesis: $CD4^+$ T cells and $CD14^+$ monocytes from SSc patients and healthy controls in an attempt to annotate gene targets within all known SSc GWAS loci. We also integrate these data with RNA-seq to create a multi-omic approach in order to identify interactomic and

transcriptomic differences between cell types and disease state that could be of interest in the pathogenesis of SSc.

## MATERIAL AND METHODS

Please see **Supplementary Material and Methods** for more details.

**Isolation of $CD4^+$ T cells and $CD14^+$ monocytes**

Primary $CD4^+$ T cells and $CD14^+$ monocytes were collected from 10 systemic sclerosis patients and 5 healthy individuals. All SSc patients were diagnosed according to the American College of Rheumatology (ACR)/European Alliance of Associations for Rheumatology (EULAR) 2013 criteria (cohorts characteristics described in **Supplementary Table 1**). All patients and
controls gave written informed consent, which was approved by local ethic committees. Peripheral blood mononuclear cells (PBMCs) were isolated from 70 ml blood samples using Ficoll density gradient centrifugation. EasySep Human $CD14^+$ Positive selection kit (StemCell Technologies, ref:17858) was used to isolate $CD14^+$ cells from PBMCs and, subsequently, Easysep $CD4^+$ T cell isolation kit (StemCell Technologies, ref:17952) was used to isolate $CD4^+$ T cells from the remaining PBMCs, according to the manufacturer's instructions.

**Promoter capture Hi-C probe design**

First, gene annotations for 18,755 protein coding genes were extracted from Ensembl's genebuild database version 97 GRCh38. Capture regions were identified by mapping the transcription start site (TSS) coordinates to the *in silico* digested (Arima Hi-C) genome and extracting the fragments containing the TSS coordinates as well as the fragments directly upstream and downstream.

**Capture Hi-C library generation**

5-10 million isolated $CD4^+$ T cells and $CD14^+$ monocytes were crosslinked in 1% formaldehyde; the reaction was then quenched with 0.125 M glycine. Each Hi-C library was prepared from fixed cells following the Arima HiC kit (Arima Genomics) and the KAPA HyperPrep kit (KAPA Biosystems) following the manufacturer's protocol. Hi-C samples were then hybridized with the SureSelect custom capture library by following Agilent SureSelectXT HS reagents (ref: G9702A, G9496A) and protocols (ref: G9702-9000).

**Promoter capture Hi-C sequencing and processing**

Sequencing for 30 prepared pCHi-C libraries was performed using Illumina NovaSeq S4 flow cell on Illumina NovaSeq6000. Subsequent mapping with GRCh38 and filtering was performed with HiCUP v0.7.4 (25) and bowtie2 v2.3.2 (Statistics in **Supplementary Table 2**). Significant chromatin interactions were identified using CHiCAGO v1.13.1 (26) using a threshold of CHiCAGO score > 5 in different conditions; cell type: $CD4^+$ T cells (n=15) and

$CD14^+$ monocytes (n=15); cell type and disease state: $CD4^+$ T cells from SSc patients (n=10) and healthy controls (n=5), and $CD14^+$ monocytes from SSc patients (n=10) and healthy controls (n=5). Principal component analysis (PCA) was performed in each cell type in order to detect potential biases (**Supplementary Figure 1**).

In order to detect enrichment of features in the interactions obtained with CHiCAGO for each cell type, narrowPeak bed files of H3K4me3 and H3K27ac were obtained. Finally, Chicdiff v0.6 (27) was used to detect differential interactions between different conditions: $CD4^+$ T cells vs $CD14^+$ monocytes; SSc patients vs healthy controls $CD4^+$ T cells; and SSc patients vs healthy controls $CD14^+$ monocytes. For each comparison, only those interactions with CHiCAGO score > 5 in at least one condition were included in differential analysis. Differential interactions with a weighted adjusted p-value < 0.05 were identified as significant. Spearman's rank-order correlation was performed to test the correlation of $\log_2$ fold change values in differential interactions between patients and controls in $CD4^+$ T cells and $CD14^+$ monocytes.

**RNA-seq library generation**

RNA isolation from a total of 0.5 million purified cells was conducted using the RNeasy microkit (QIAGEN, ref: 74004) reagents and protocol. Libraries for RNA-seq were prepared using Illumina Truseq Stranded Total RNA reagents and protocol, except for Control 1 $CD4^+$ and $CD14^+$ samples, for which library preparation failed. The 28 libraries generated were sequenced on Illumina HiSeq4000.

**RNA-seq data processing**

Reads were mapped using STAR v2.7.3a on the GRCh38 genome with GENCODE annotation v32. Reads were de-duplicated and then counted (**Supplementary Table 3**). Final count matrices were analysed using edgeR v3.28.1 to perform normalization and differential expression analysis. Differentially expressed genes were called with an adjusted p-value of 0.1 (FDR 10%). Functional enrichment analyses were performed with g:Profiler (28) with default settings.

**Linking differential expression and differential interactions in $CD4^+$ T cells vs $CD14^+$ monocytes**

Genes corresponding with the promoter end of significant differential interactions observed between $CD4^+$ and $CD14^+$ cells were overlapped with those differentially expressed. One-sided Fisher's exact test was performed in order to calculate the enrichment of genes with differential interactions in those differentially expressed. In this set of overlapping genes, Spearman's rank-order correlation was performed to test the correlation of $\log_2$ fold change values in differential interactions and differential expression. Finally, in order to test the distribution of $\log_2$ fold change values, a binomial exact test was performed on a subset of overlapping genes obtained adding a more stringent cutoff (absolute value of median $\log_2$FC > 2 for each gene). Functional enrichment analyses were performed with g:Profiler (28) with default settings.

**Defining SSc GWAS loci**

All independent non-MHC disease-associated signals for SSc were selected from the largest meta-GWAS performed to date (9). We defined 23 regions based on linkage disequilibrium data and SNP proximity from the total of 27 independent signals described in GWAS. The window ranges and total number of SNPs in each of the 23 final loci are specified in **Supplementary Table S4**.

**Defining enhancers and TADs in $CD4^+$ T cells and $CD14^+$ monocytes**

In order to define enhancer regions, chromHMM v1.22 annotations from 9 $CD4^+$ T cells and 4 $CD14^+$ monocytes were downloaded from the EpiMap project (29). For each cell type, enhancer regions were defined as those with state number from chromHMM corresponding to enhancer activity present in at least one sample. TADs definition for $CD4^+$ T cells and $CD14^+$ monocytes were obtained from Javierre et al. (22).

**Overlap between pCHi-C, SSc GWAS loci, and enhancer regions**

In order to prioritize certain interactions observed in pCHi-C data of particular interest in SSc GWAS loci, the SNP set previously defined in "Defining SSc GWAS loci" was overlapped with enhancer regions of each cell type (**Supplementary Table 4**). This new SNP set was then overlapped with the promoter interacting regions (PIRs) of significant pCHi-C interactions, defining candidate interacting genes as those in which their PIR overlaps with our significant SSc SNP set and enhancer regions. One-sided Fisher's exact test was performed in order to calculate the enrichment of the SNP set in $CD4^+$ T cells and $CD14^+$ monocytes enhancer regions. A z-test was performed to calculate the enrichment of SNPs overlapping enhancer regions between cell types. Functional enrichment analyses were performed for the sets of interacting genes observed in $CD4^+$ T cells and $CD14^+$ monocytes with g:Profiler (28).

**Visualization tools**

The WashU Epigenome browser was used to plot pCHi-C interactions, enhancer regions defined by chromHMM and H3K27ac peaks (from EpiMap (29) samples previously defined), and TADs (from Javierre et al. (22)) in $CD4^+$ T cells and $CD14^+$ monocytes.

**Drug target analysis**

In order to assess if genes interacting with SSc GWAS loci in $CD4^+$ T cells and $CD14^+$ monocytes presented potential drug targets that could be repurposed for its use in SSc, those genes interacting with PIR overlapping significant SSc GWAS SNPs and enhancer regions, were used to model a protein-protein interaction (PPI) network using STRING v11 (30) (**Supplementary Table 5**). Protein products from these genes and those in direct PPI with them were used to query the OpenTargets Platform for drug targets. Additionally, the same platform and the Drugbank database were searched for information on clinical studies of drug targets of interest in SSc.

# RESULTS

We generated pCHi-C data for $CD4^+$ T cells and $CD14^+$ monocytes from 10 SSc patients and 5 healthy controls. CHiCAGO was used to identify significant promoter interactions (CHiCAGO score>5) for each cell type and disease condition (**Supplementary Table 6**) and Chicdiff was used to identify differential interactions between cell types, and between disease conditions for each cell type. A total of 81,624 and 74,853 significant interactions corresponding to 8,193 and 7,024 captured promoters were identified in $CD4^+$ T cells and $CD14^+$ monocytes, respectively. In addition, 71,213 significant differential interactions (weighted adjusted p-value<0.05) corresponding to 8,223 captured promoters were obtained in the comparison between cell types. Through integration with published ChIP-seq data, we found that PIRs were enriched in H3K27ac and H3K4me3 histone marks from primary $CD4^+$ naive T cells and $CD14^+$ monocytes (**Supplementary Figure 2**), suggesting that promoters mostly interact with regulatory active regions such as enhancers.

**Differential interactions and expression between SSc patients and healthy controls**

One of the aims of our study was to identify specific interactions that could be present in SSc patients but not in healthy controls, or vice versa, and thus, identify specific genes interacting with enhancer regions and SSc GWAS loci that could be of interest in SSc pathology. We identified a total of 4,858 significant differential interactions (weighted adjusted p-value<0.05) between SSc patients and healthy controls in $CD4^+$ T cells, corresponding to 1,526 captured promoters, although the significance was modest (median weighted adjusted p-value=$2.2x10^{-2}$) as compared with differential interactions between cell types (median weighted adjusted p-value=$2.16x10^{-10}$). However, we could not detect any significant differential interactions in $CD14^+$ monocytes. On the other hand, none of the 23 SSc GWAS associated regions showed significant differences at the interaction level between patients and controls. Besides, we identified a total of 62 and 63 differentially expressed genes (FDR < 0.05) between patients and controls in $CD4^+$ T cells and $CD14^+$ monocytes, respectively (**Supplementary Tables 7** and **8**). In the case of $CD4^+$ T cells we observed significant enrichment in terms related with immune response such as “positive regulation of immune system process” or “leukocyte activation” (**Supplementary Table 9**). However, we could not identify any functional enrichment regarding the 63 genes differentially expressed in $CD14^+$ monocytes.

**Linking differential expression and differential interactions in $CD4^+$ T cells vs $CD14^+$ monocytes**

We decided to look at differences at the interaction and expression levels between cell types, without taking disease state into account. On this subject, a total of 19,125 protein coding genes were analyzed in the RNA-seq data, of which 9,795 were identified as differentially expressed between $CD4^+$ T cells and $CD14^+$ monocytes. Subsequently, 2,257 strongly differentially expressed genes were obtained (FDR<0.05, $|\log_2 FC|>2$), of which 919 and 1,338 genes were overexpressed in $CD4^+$ T cells and $CD14^+$ monocytes, respectively. Overrepresentation analyses showed that each group of genes is, as expected, significantly

enriched in terms related with T cells and monocytes specific pathways, including gene ontology terms such as "T cell activation" and "T cell differentiation" in $CD4^+$ T cells, and "leukocyte activation" in $CD14^+$ monocytes (**Supplementary Tables 10** and **11**). In addition, we observed that differentially expressed genes are in fact significantly enriched in differentially interacting genes (fisher exact test p-value=$3.54x10^{-37}$, OR=1.77). Furthermore, from the total of 1,209 differentially expressed genes overlapping differentially interacting genes, we observed that genes overexpressed in a specific cell type significantly correlated with increased number of interactions in that cell type, and vice versa (Spearman's rank correlation p-value=$1.04x10^{-197}$, rho=0.73). Finally, we applied a more stringent cutoff in differentially interacting genes ($|log_2FC|>2$), leading to a total of 97 differentially expressed genes overlapping differentially interacting genes. In this subset, only 2 of the 97 genes were not distributed as expected; whilst 23 and 72 genes were overexpressed and presented an increased number of interactions in $CD4^+$ T cells and $CD14^+$ monocytes, respectively (exact binomial test p-value=$6.01x10^{-26}$, probability of success=98%) (**Supplementary Figure 3**). Thus, our results demonstrate the importance of using different cell types to define promoter interactions and how they are linked with the expression of important genes for those cell types. In this regard, we decided to define significant interactions that linked SSc GWAS loci with promoters in $CD4^+$ T cells and $CD14^+$ monocytes.

**SSc GWAS loci and $CD4^+$ / $CD14^+$ promoter interactions**

To identify new potential target genes associated to SSc, as well as the potential implication of different cell types in those associations, we performed a multi-omic approach overlapping 23 regions defined based on the most powerful SSc meta-GWAS performed to date (9) with enhancer regions and our pCHi-C data (see online **Supplementary Material and Methods** for more detail). From the total of 1,505 SNPs corresponding to genome-wide significant (p-value<$5x10^{-8}$) SNPs associated with SSc and those in high linkage disequilibrium ($r^2>0.8$) with them, 445 (29.6%) and 284 (18.9%) overlapped with enhancer regions from $CD4^+$ T cells and $CD14^+$ monocytes, respectively. As expected, the GWAS SNP set was significantly enriched in both $CD4^+$ and $CD14^+$ enhancer regions (one-sided Fisher's exact test p-value=$5.91x10^{-133}$, OR=4.86 in $CD4^+$ T cells; p-value=$1.63x10^{-56}$, OR=3.27 in $CD14^+$ monocytes). In addition, the differences in the number of SNPs overlapping $CD4^+$ and $CD14^+$ enhancer regions were significant (two proportion z-test p-value=0.001), observing a stronger overlap with $CD4^+$ T cell enhancer regions as compared with those from $CD14^+$ monocytes. These GWAS SNPs within enhancer regions were overlapped with PIRs from pCHi-C, obtaining a total of 398 and 109 significant interactions in $CD4^+$ T cells and $CD14^+$ monocytes, respectively (**Supplementary Table 4**). The promoter ends of those interactions correspond to 46 genes, with a total of 40 and 27 interacting genes in $CD4^+$ T cells and $CD14^+$ monocytes, respectively (**Table 1**).

The physical interaction maps presented here identify 39 new potential candidate genes and confirm 7 genes which have been associated by classical GWAS methods using proximity. Differential expression and differential interaction data for each of the 46 genes and baited promoters are available in **Supplementary Tables 12** and **13**, respectively. Interestingly, some SSc confirmed genes such as *IRF8*, *STAT4*, or *CD247*, showed cell type specific

interactions (**Figures 1-3**). The *IRF8* locus (**Figure 1**) provides a good example in which interactions between SNPs overlapping enhancer regions (represented by H3K27ac mark peaks) and *IRF8* promoter are exclusively found in one cell type and are associated to differential gene expression between cells, in this case corresponding to $CD14^+$ monocytes, that showed a much higher expression of *IRF8* ($log_2FC$=-4.47, FDR=$3.11x10^{-72}$). In the case of *STAT4* (**Figure 2**), significant interactions with the *STAT4* promoter were identified exclusively in $CD4^+$ T cells, corresponding with a TAD specific for $CD4^+$ T cells that is not found in monocytes. In addition, *STAT4* showed a significantly higher expression in $CD4^+$ T cells as compared with $CD14^+$ monocytes ($log_2FC$=7.05, FDR=$1x10^{-304}$). Cell type specific interactions are also observed in the *CD247* GWAS locus (**Figure 3**), in which significant interactions between SNPs and *CD247* promoter are identified only in $CD4^+$ T cells, with an increased expression of this gene in $CD4^+$ T cells as compared with $CD14^+$ monocytes ($log_2FC$=7.49, FDR=$3.99x10^{-210}$).

On the other hand, we identified new potential candidate genes interacting with SSc GWAS associated SNPs, like the *DDX6* locus (**Figure 4**) in which we found significant interactions between SNPs overlapping enhancer regions and not only *DDX6*, but also other potential candidate genes including *CXCR5*, *UPK2*, and *IFT46/ARCN1* promoters in $CD4^+$ T cells. In $CD14^+$ monocytes, only a significant interaction with *CXCR5* promoter was found. All of these interactions are intra-TAD, except for the one including *IFT46/ARCN1* promoters, and we observed a significantly higher gene expression of *CXCR5* ($log_2FC$=3.21, FDR=$1.05x10^{-09}$) and *DDX6* ($log_2FC$=1.14, FDR=$2.38x10^{-83}$) in $CD4^+$ T cells, while *ARCN1* showed a slight overexpression in $CD14^+$ monocytes ($log_2FC$=-0.21, FDR=$3.69x10^{-03}$).

In order to identify what pathways could be driving disease in the two different cell types, we performed a functional enrichment analysis including the genes interacting with SSc GWAS loci for each cell type. In $CD4^+$ T cells, the set of 40 interacting genes observed showed enrichment in virus response and pancreatic carcinoma (**Supplementary Table 14**). In accordance with this, a higher incidence of cancer in SSc patients compared with the general population has been suggested in several studies (31). On the other hand, the set of 27 interacting genes observed in $CD14^+$ monocytes showed enrichment in tyrosine kinase activity (**Supplementary Table 15**), which plays an important role in fibrosis, and has been related with SSc pathogenesis, being tyrosine kinase inhibitors one of the most promising antifibrotic therapies for SSc and other fibrotic diseases (32).

Interaction plots of the rest of SSc GWAS loci in $CD4^+$ T cells and $CD14^+$ monocytes can be found in **Supplementary Figures 4-22**.

**Drug repurposing in SSc**

From the 46 genes that present PIRs overlapping significant SSc GWAS SNPs and enhancer regions, we identified a total of 21 drugs with interest in SSc targeting protein products in strong protein-protein interaction (PPI) with 13 of those genes (5 of them specific for $CD4^+$ T cells interactions) (**Table 2**). Fifteen of these drugs correspond to potential drug targets already in use, or at least in completed clinical phase III, in other similar immune-mediated

diseases that could be repurposed for SSc treatment, such as metformin or dimethyl fumarate. Apart from new potential drug targets, tocilizumab and nintedanib were two of the drugs highlighted in our analysis, both of them approved by Food and Drug Administration (FDA) for its use in SSc-associated interstitial lung disease (33,34). We also identified 4 drugs which present advanced clinical trials developed in SSc (tofacitinib, bosentan, methylprednisolone and mycophenolic acid).

## DISCUSSION

Our investigation integrates four dimensions in the study of SSc genetics; GWAS, chromosome conformation, gene expression, and cell-specificity. In this regard, our findings stress the importance of cell type in the functional interpretation of GWAS associations. We identified new target genes, and confirmed others, in SSc GWAS loci in two of the main cell types associated with the disease, $CD4^+$ T cells and $CD14^+$ monocytes.

One of the new candidate genes observed in pCHi-C data corresponds to CXC chemokine receptor type 5 (*CXCR5*) in the *DDX6* GWAS locus (**Figure 4**). *CXCR5* plays an important role in the differentiation of follicular helper T (Tfh) cells, and is highly expressed in $CD4^+$ and $CD8^+$ T cells (35). In addition, a recently published study observed that Tfh cells ($CD4^+CXCR5^+PD\text{-}1^+$) are increased in systemic sclerosis, and correlate with SSc severity (36). In line with the above, interactions with the promoter of this gene were identified specifically in $CD4^+$ T cells in our study, and transcript levels showed an upregulation in this cell type. Furthermore, *CXCR5* has been associated through GWAS studies in other similar immune-mediated diseases, such as rheumatoid arthritis or inflammatory bowel disease (37,38). Thus, *CXCR5* represents a good candidate gene contributing to SSc pathology, with a particular interest in $CD4^+$ T cells. Another interesting example is found in the *RAB2A-CHD7* locus, a recently discovered locus associated with SSc (9) (**Supplementary Figure 16**). Within this region, we observed significant interactions between SSc GWAS SNPs and the closest gene, *CHD7*, in $CD4^+$ T cells. *CHD7* is a chromatin remodeler that has been associated with lymphocyte (and other immune-related cells) counts in blood through GWAS (39). Regarding the *IL12A* locus (**Supplementary Figure 9**), we identified long-range interactions between SSc GWAS SNPs and the promoter of *SMC4* in $CD14^+$ monocytes. *SMC* family genes play a central role in organizing and compacting chromosomes. In this line, a recent study showed *SMC4* promotes an inflammatory innate immune response, which is directly associated with monocyte activity, through enhancing NEMO transcription, an essential modulator of NF-Kb (40). Although *IL12A* has been traditionally set as the most probable candidate gene for this association, we did not observe any interactions between SSc GWAS SNPs and the promoter of this gene. Here, it is important to note the increased difficulty to identify significant short-range interactions (<1 Mb) as background read count levels are dependent on the distance between fragments (26). This phenomenon represents a limitation in this kind of studies, as most of the GWAS SNPs are classically related with the closest gene, being these SNPs located within the gene itself in some cases. In this sense, new

high resolution Hi-C methods should help overcome the limitation of detecting very short range interactions (41).

Regarding previously confirmed genes associated with SSc, we described interactions between *IRF8* promoter and SSc GWAS SNPs that were only present in $CD14^+$ monocytes (**Figure 1**), corresponding with an upregulated expression of this gene in $CD14^+$ monocytes as compared with $CD4^+$ T cells. This transcription factor plays an important role in differentiation and regulation of monocytes and macrophages (42). Furthermore, variants in *IRF8* have been associated with monocyte counts across different populations (43), and a downregulation of *IRF8* in monocytes and macrophages of SSc patients that may affect the fibrotic phenotype of the disease was reported (44). A recent study demonstrated that the deletion of an enhancer region corresponding with our SSc GWAS locus in mice model decreased *Irf8* expression, resulting in an overproduction of inflammatory $Ly6c^+$ monocytes (45). Thus, our results confirm the association of *IRF8* with SSc through physical chromatin interactions particularly in $CD14^+$ monocytes. In the same line, *CD247* and *STAT4* have been described in many previous GWAS studies as main candidate genes associated with SSc (9,10), in this case interactions were exclusively found in $CD4^+$ T cells (**Figures 2-3**). These findings are in line with literature, as both genes play an important role particularly in T cell signaling and differentiation (46,47). Thus, our results highlight the importance of associating GWAS signals with the specific cell types in which interactions are found, acting as a lead starting point for follow-up functional studies that can relate these signals with the disease.

Our results reveal that 3D chromatin structure is largely preserved between SSc patients and healthy controls at least in $CD4^+$ T cells and $CD14^+$ monocytes, which make them difficult to interpret. So far, there is only one published study in which authors attempt to observe differences at the interaction level between patients and healthy controls in $CD4^+$ T cells from juvenile idiopathic arthritis patients (48). However, no differences at the interactomic level were observed, which supports our hypothesis and underlines the difficulty to describe these subtle differences with current technology. Interestingly, it has been shown that subtle differences in chromatin interactions may be correlated with large functional effects on gene expression (49). Thus, larger studies would be of great interest to uncover the importance of these differences in understanding the implication of different cell types in disease pathology.

Furthermore, we wanted to describe general differences between cell types at the interaction and expression level. We observed that overexpressed genes in a specific cell type correlated with an increased number of interactions, and that those genes were enriched in specific pathways related with T cells and monocytes signaling, activation, and differentiation. These results demonstrate that interactions are directly related with the expression of important genes implicated in cell type specific pathways. In this regard, a recent study observed that disease-associated genes tend to be connected by cell-type-specific interactions (50). Thus, our data presented here will aid future studies to identify cell types enriched with interactions overlapping GWAS loci.

## ACKNOWLEDGEMENTS

We greatly acknowledge the expert technical assistance of Sofía Vargas Roldán at the Institute of Parasitology and Biomedicine López-Neyra [IPBLN]–CSIC, as well as the assistance given by Information Technology Services and the use of the Computational Shared Facility at The University of Manchester, United Kingdom. This work is part of the Doctoral Thesis "Deciphering the genomic architecture of systemic sclerosis".

## COMPETING INTEREST

Authors declare no competing interests.

## DATA AVAILABILITY STATEMENT

Data are available upon reasonable request. All data relevant to the study are included in the article or uploaded as supplementary data.

## REFERENCES


1. Denton CP, Khanna D. Systemic sclerosis. Lancet. 2017;390(10103):1685–99.

2. Brown M, O'Reilly S. The immunopathogenesis of fibrosis in systemic sclerosis. Clin Exp Immunol. 2019;195(3):310–21.

3. Stifano G, Christmann RB. Macrophage Involvement in Systemic Sclerosis: Do We Need More Evidence? Curr Rheumatol Reports. 2015;18(1):1–6.

4. Pillai S. T and B lymphocytes in fibrosis and systemic sclerosis. Curr Opin Rheumatol. 2019;31(6):576–81.

5. Fuschiotti P. T cells and cytokines in systemic sclerosis. Curr Opin Rheumatol. 2018;30(6):594–9.

6. Bhandari R, Ball MS, Martyanov V, Popovich D, Schaafsma E, Han S, et al. Profibrotic Activation of Human Macrophages in Systemic Sclerosis. Arthritis Rheumatol. 2020;72(7):1160–9.

7. Soldano S, Trombetta AC, Contini P, Tomatis V, Ruaro B, Brizzolara R, et al. Increase in circulating cells coexpressing M1 and M2 macrophage surface markers in patients with systemic sclerosis. Ann Rheum Dis. 2018;77(12):1842–5.

8. Moreno-Moral A, Bagnati M, Koturan S, Ko J-H, Fonseca C, Harmston N, et al. Changes in macrophage transcriptome associate with systemic sclerosis and mediate GSDMA contribution to disease risk. Ann Rheum Dis. 2018;77(4):596–601.

9. López-Isac E, Acosta-Herrera M, Kerick M, Assassi S, Satpathy AT, Granja J, et al. GWAS for systemic sclerosis identifies multiple risk loci and highlights fibrotic and vasculopathy pathways. Nat Commun. 2019;10(1):1–14.

10. Radstake TRDJ, Gorlova O, Rueda B, Martin JE, Alizadeh BZ, Palomino-Morales R, et al. Genome-wide association study of systemic sclerosis identifies CD247 as a new susceptibility locus. Nat Genet. 2010;42(5):426–9.

11. Bossini-Castillo L, López-Isac E, Martín J. Immunogenetics of systemic sclerosis: Defining heritability, functional variants and shared-autoimmunity pathways. J Autoimmun. 2015;64:53–65.

12. Orvain C, Assassi S, Avouac J, Allanore Y. Systemic sclerosis pathogenesis: contribution of recent advances in genetics. Curr Opin Rheumatol. 2020;32(6):505–14.

13. Acosta-Herrera M, López-Isac E, Martín J. Towards a Better Classification and Novel Therapies Based on the Genetics of Systemic Sclerosis. Curr Rheumatol Rep. 2019;21(9):1–7.

14. Farh KK-H, Marson A, Zhu J, Kleinewietfeld M, Housley WJ, Beik S, et al. Genetic and epigenetic fine mapping of causal autoimmune disease variants. Nature. 2014;518(7539):337–43.

15. Poppenberg KE, Tutino VM, Tarbell E, Jarvis JN. Broadening our understanding of genetic risk for scleroderma/systemic sclerosis by querying the chromatin architecture surrounding the risk haplotypes. BMC Med Genomics. 2021 Apr 24;14(1):1–12.

16. Rao SSP, Huntley MH, Durand NC, Stamenova EK, Bochkov ID, Robinson JT, et al. A 3D Map of the Human Genome at Kilobase Resolution Reveals Principles of Chromatin Looping. Cell. 2014;159(7):1665–80.

17. Ding J, Frantzeskos A, Orozco G. Functional genomics in autoimmune diseases. Hum Mol Genet. 2020;29(R1):R59–65.

18. Dekker J, Rippe K, Dekker M, Kleckner N. Capturing chromosome conformation. Science. 2002;295(5558):1306–11.

19. Lieberman-Aiden E, Van Berkum NL, Williams L, Imakaev M, Ragoczy T, Telling A, et al. Comprehensive mapping of long-range interactions reveals folding principles of the human genome. Science. 2009;326(5950):289–93.

20. Belton JM, McCord RP, Gibcus JH, Naumova N, Zhan Y, Dekker J. Hi–C: A comprehensive technique to capture the conformation of genomes. Methods. 2012;58(3):268–76.

21. Schoenfelder S, Javierre B-M, Furlan-Magaril M, Wingett SW, Fraser P. Promoter Capture Hi-C: High-resolution, Genome-wide Profiling of Promoter Interactions. Journal Vis Exp. 2018;2018(136):e57320.

22. Javierre BM, Burren OS, Wilder SP, Kreuzhuber R, Hill SM, Sewitz S, et al. Lineage-Specific Genome Architecture Links Enhancers and Non-coding Disease Variants to Target Gene Promoters. Cell. 2016;167(5):1369-1384.e19.

23. Martin P, McGovern A, Orozco G, Duffus K, Yarwood A, Schoenfelder S, et al. Capture Hi-C reveals novel candidate genes and complex long-range interactions with related autoimmune risk loci. Nat Commun. 2015;6(1):1–7.

24. Martin P, Ding J, Duffus K, Gaddi VP, McGovern A, Ray-Jones H, et al. Chromatin interactions reveal novel gene targets for drug repositioning in rheumatic diseases. Ann Rheum Dis. 2019;78(8):1127–34.

25. Wingett S, Ewels P, Furlan-Magaril M, Nagano T, Schoenfelder S, Fraser P, et al. HiCUP: pipeline for mapping and processing Hi-C data. F1000Research. 2015;4.

26. Cairns J, Freire-Pritchett P, Wingett SW, Várnai C, Dimond A, Plagnol V, et al. CHiCAGO: robust detection of DNA looping interactions in Capture Hi-C data. Genome Biol. 2016;17(1):1–17.

27. Cairns J, Orchard WR, Malysheva V, Spivakov M. Chicdiff: a computational pipeline for detecting differential chromosomal interactions in Capture Hi-C data. Bioinformatics. 2019;35(22):4764–6.

28. Raudvere U, Kolberg L, Kuzmin I, Arak T, Adler P, Peterson H, et al. g:Profiler: a web server for functional enrichment analysis and conversions of gene lists (2019 update). Nucleic Acids Res. 2019;47(W1):W191–8.

29. Boix CA, James BT, Park YP, Meuleman W, Kellis M. Regulatory genomic circuitry of human disease loci by integrative epigenomics. Nature. 2021;590(7845):300–7.

30. Szklarczyk D, Gable AL, Lyon D, Junge A, Wyder S, Huerta-Cepas J, et al. STRING v11: Protein-protein association networks with increased coverage, supporting functional discovery in genome-wide experimental datasets. Nucleic Acids Res. 2019;47(D1):D607–13.

31. Bonifazi M, Tramacere I, Pomponio G, Gabrielli B, Avvedimento E V., La Vecchia C, et al. Systemic sclerosis (scleroderma) and cancer risk: systematic review and meta-analysis of observational studies. Rheumatology. 2013;52(1):143–54.

32. Mendoza FA, Piera-Velazquez S, Jimenez SA. Tyrosine kinases in the pathogenesis of tissue fibrosis in systemic sclerosis and potential therapeutic role of their inhibition. Transl Res. 2021;231:139–58.

33. Genetech Inc. Genentech's Actemra Becomes the First Biologic Therapy Approved by the FDA for Slowing the Rate of Decline in Pulmonary Function in Adults With Systemic Sclerosis-Associated Interstitial Lung Disease, a Rare, Debilitating Condition . 2021. Available from: https://www.gene.com/media/press-releases/14897/2021-03-04/genentechs-actemra-becomes-the-first-bio

34. FDA approves first treatment for patients with rare type of lung disease | FDA. 2019. Available from: https://www.fda.gov/news-events/press-announcements/fda-approves-first-treatment-patients-rare-type-lung-disease

35. Moser B. CXCR5, the Defining Marker for Follicular B Helper T (TFH) Cells. Front Immunol. 2015;0:296.

36. Ricard L, Jachiet V, Malard F, Ye Y, Stocker N, Rivière S, et al. Circulating follicular helper T cells are increased in systemic sclerosis and promote plasmablast differentiation through the IL-21 pathway which can be inhibited by ruxolitinib. Ann Rheum Dis. 2019;78(4):539–50.

37. Okada Y, Wu D, Trynka G, Raj T, Terao C, Ikari K, et al. Genetics of rheumatoid arthritis contributes to biology and drug discovery. Nature. 2013;506(7488):376–81.

38. Jostins L, Ripke S, Weersma RK, Duerr RH, McGovern DP, Hui KY, et al. Host–microbe interactions have shaped the genetic architecture of inflammatory bowel disease. Nature. 2012;491(7422):119–24.

39. Astle WJ, Elding H, Jiang T, Allen D, Ruklisa D, Mann AL, et al. The Allelic Landscape of Human Blood Cell Trait Variation and Links to Common Complex Disease. Cell. 2016;167(5):1415-1429.e19.

40. Wang Q, Wang C, Li N, Liu X, Ren W, Wang Q, et al. Condensin Smc4 promotes inflammatory innate immune response by epigenetically enhancing NEMO transcription. J Autoimmun. 2018;92:67–76.

41. Hua P, Badat M, Hanssen LLP, Hentges LD, Crump N, Downes DJ, et al. Defining genome architecture at base-pair resolution. Nature. 2021;595(7865):125–9.

42. Salem S, Salem D, Gros P. Role of IRF8 in immune cells functions, protection against infections, and susceptibility to inflammatory diseases. Hum Genet. 2020;139(6):707–21.

43. Crosslin DR, McDavid A, Weston N, Zheng X, Hart E, de Andrade M, et al. Genetic variation associated with circulating monocyte count in the eMERGE Network. Hum Mol Genet. 2013;22(10):2119–27.

44. Ototake Y, Yamaguchi Y, Asami M, Komitsu N, Akita A, Watanabe T, et al. Downregulated IRF8 in Monocytes and Macrophages of Patients with Systemic Sclerosis May Aggravate the Fibrotic Phenotype. J Invest Dermatol. 2021;141(8):1954–63.

45. Murakami K, Sasaki H, Nishiyama A, Kurotaki D, Kawase W, Ban T, et al. A RUNX–CBFβ-driven enhancer directs the Irf8 dose-dependent lineage choice between DCs and monocytes. Nat Immunol. 2021;22(3):301–11.

46. Irving BA, Chan AC, Weiss A. Functional characterization of a signal transducing motif present in the T cell antigen receptor zeta chain. J Exp Med. 1993;177(4):1093–103.

47. O'Shea JJ, Lahesmaa R, Vahedi G, Laurence A, Kanno Y. Genomic views of STAT function in CD4+ T helper cell differentiation. Nat Rev Immunol. 2011;11(4):239–50.

48. Tarbell E, Jiang K, Hennon TR, Holmes L, Williams S, Fu Y, et al. CD4+ T cells from children with active juvenile idiopathic arthritis show altered chromatin features associated with transcriptional abnormalities. Sci Reports. 2021;11(1):1–14.

49. Greenwald WW, Li H, Benaglio P, Jakubosky D, Matsui H, Schmitt A, et al. Subtle changes in chromatin loop contact propensity are associated with differential gene regulation and expression. Nat Commun. 2019;10(1):1–17.

50. Mohammadi S, Davila-Velderrain J, Kellis M. Reconstruction of Cell-type-Specific Interactomes at Single-Cell Resolution. Cell Syst. 2019;9(6):559-568.e4.

## FIGURE LEGENDS

**Figure 1.**

Promoter capture Hi-C (pCHi-C) interactions and gene expression in the *IRF8* GWAS locus. (**A**) Genomic coordinates (GRCh38) are shown at the top of the panel. The tracks include RefSeq genes (NCBI), systemic sclerosis (SSc) GWAS SNPs from López-Isac et al.(9) and those in high linkage disequilibrium (LD) ($r^2$>0.8), TADs (shown as bars), SNPs overlapping promoter interacting regions (PIRs) and enhancer regions, enhancer regions as defined by chromHMM, H3K27ac signal, and pCHi-C significant interactions (CHiCAGO score > 5) (shown as arcs) in $CD4^+$ T cells (blue) and $CD14^+$ monocytes (red). The highlighted region in red includes all the systemic sclerosis (SSc) SNPs LD block. (**B**) Gene expression level of *IRF8* from $CD4^+$ T cells and $CD14^+$ monocytes in counts per million (CPM). (**C**) Chicdiff bait profiles were generated for *IRF8* gene. The plot shows the raw read counts versus linear distance from the bait fragment as mirror images for $CD4^+$ T cells and $CD14^+$ monocytes. Other-end interacting fragments are pooled and color-coded by their adjusted weighted p-value. Significant differentially interacting regions detected by Chicdiff overlapping SSc GWAS SNPs and enhancer regions are depicted as red blocks.

**Figure 2.**

Promoter capture Hi-C (pCHi-C) interactions and gene expression in the *STAT4* GWAS locus. (**A**) Genomic coordinates (GRCh38) are shown at the top of the panel. The tracks include RefSeq genes (NCBI), systemic sclerosis (SSc) GWAS SNPs from López-Isac et al.(9) and those in high linkage disequilibrium (LD) ($r^2$>0.8), TADs (shown as bars), SNPs overlapping promoter interacting regions (PIRs) and enhancer regions, enhancer regions as defined by chromHMM, H3K27ac signal, and pCHi-C significant interactions (CHiCAGO score > 5) (shown as arcs) in $CD4^+$ T cells (blue) and $CD14^+$ monocytes (red). The highlighted region in red includes all the systemic sclerosis (SSc) SNPs LD block. (**B**) Gene expression level of *STAT4* and *NABP1* from $CD4^+$ T cells and $CD14^+$ monocytes in counts per million (CPM). (**C**) Chicdiff bait profiles were generated for *STAT4* and *NABP1* genes. Plots show the raw read counts versus linear distance from the bait fragment as mirror images for $CD4^+$ T cells and $CD14^+$ monocytes. Other-end interacting fragments are pooled and color-coded by their adjusted weighted p-value. Significant differentially interacting regions

detected by Chicdiff overlapping SSc GWAS SNPs and enhancer regions are depicted as red blocks.

**Figure 3.**

Promoter capture Hi-C (pCHi-C) interactions and gene expression in the *CD247* GWAS locus. (**A**) Genomic coordinates (GRCh38) are shown at the top of the panel. The tracks include RefSeq genes (NCBI), systemic sclerosis (SSc) GWAS SNPs from López-Isac et al.(9) and those in high linkage disequilibrium (LD) ($r^2$>0.8), TADs (shown as bars), SNPs overlapping promoter interacting regions (PIRs) and enhancer regions, H3K27ac signal, enhancer regions as defined by chromHMM, and pCHi-C significant interactions (CHiCAGO score > 5) (shown as arcs) in $CD4^+$ T cells (blue) and $CD14^+$ monocytes (red). The highlighted region in red includes all the systemic sclerosis (SSc) SNPs LD block. (**B**) Gene expression level of *CD247* and *CREG1* from $CD4^+$ T cells and $CD14^+$ monocytes in counts per million (CPM). (**C**) Chicdiff bait profiles were generated for *CD247* and *CREG1* genes. Plots show the raw read counts versus linear distance from the bait fragment as mirror images for $CD4^+$ T cells and $CD14^+$ monocytes. Other-end interacting fragments are pooled and color-coded by their adjusted weighted p-value. Significant differentially interacting regions detected by Chicdiff overlapping SSc GWAS SNPs and enhancer regions are depicted as red blocks.

**Figure 4.**

Promoter capture Hi-C (pCHi-C) interactions and gene expression in the *DDX6* GWAS locus. (**A**) Genomic coordinates (GRCh38) are shown at the top of the panel. The tracks include RefSeq genes (NCBI), systemic sclerosis (SSc) GWAS SNPs from López-Isac et al.(9) and those in high linkage disequilibrium (LD) ($r^2$>0.8), TADs (shown as bars), SNPs overlapping promoter interacting regions (PIRs) and enhancer regions, enhancer regions as defined by chromHMM, H3K27ac signal, and pCHi-C significant interactions (CHiCAGO score > 5) (shown as arcs) in $CD4^+$ T cells (blue) and $CD14^+$ monocytes (red). The highlighted region in red includes all the systemic sclerosis (SSc) SNPs LD block. (**B**) Gene expression level of *CXCR5*, *DDX6*, *ARCN1*, and *IFT46* from $CD4^+$ T cells and $CD14^+$ monocytes in counts per million (CPM). (**C**) Chicdiff bait profiles were generated for *CXCR5*, *DDX6*, *IFT46/ARCN1* (shared capture bait), and *UPK2* genes. Plots show the raw read counts versus linear distance from the bait fragment as mirror images for $CD4^+$ T cells and $CD14^+$ monocytes. Other-end interacting fragments are pooled and color-coded by their adjusted weighted p-value. Significant differentially interacting regions detected by Chicdiff overlapping SSc GWAS SNPs and enhancer regions are depicted as red blocks.

# TABLES

**Table 1. Promoter capture Hi-C target genes for the 23 systemic sclerosis associated regions in CD4$^+$ T cells and CD14$^+$ monocytes**

| | | | pCHi-C target genes[3] | | CD4$^+$ vs CD14$^+$ | |
|---|---|---|---|---|---|---|
| **Chr** | **Bp (start - end)[1]** | **GWAS Locus[2]** | **CD4$^+$ T cells** | **CD14$^+$ monocytes** | **Differential interactions** | **Differential expression** |
| 1 | 67326053 - 67448804 | *IL12RB2* | | | | |
| 1 | 167445635 - 167465040 | *CD247* | ***CD247***, *CREG1* | | ***CD247***, *CREG1* | ***CD247***, *CREG1* |
| 1 | 173337507 - 173391947 | *TNFSF4- LOC100506023 - PRDX6* | | | | |
| 2 | 190642047 - 190698201 | *NAB1* | *MFSD6, NEMP2* | *MFSD6, NEMP2, HIBCH;INPP1* | *MFSD6, NEMP2, HIBCH;INPP1* | *MFSD6, NEMP2, HIBCH, INPP1* |
| 2 | 191035723 - 191108308 | *STAT4* | ***STAT4***, *NABP1* | | ***STAT4***, *NABP1* | ***STAT4***, *NABP1* |
| 3 | 58084620 - 58482701 | *FLNB -DNASE1L3-PXK* | *RPP14, KCTD6* | *RPP14, KCTD6* | *RPP14, KCTD6* | *KCTD6* |
| 3 | 119384733 - 119546340 | *POGLUT1-TIMMDC1-CD80-ARHGAP31* | *TMEM39A;POGLUT1* | | *TMEM39A;POGLUT1* | *TMEM39A, POGLUT1* |
| 3 | 160002484 - 160030580 | *IL12A* | | *SMC4;IFT80* | *SMC4;IFT80* | *SMC4, IFT80* |
| 4 | 960523 - 990021 | *DGKQ* | *GAK;TMEM175, FGFRL1* | *GAK;TMEM175, FGFRL1* | *FGFRL1* | *GAK, TMEM175 FGFRL1* |
| 4 | 102477892 - 102615256 | *NFKB1* | *SLC39A8,* ***NFKB1****, UBE2D3;CISD2, SLC9B1, BDH2* | *SLC39A8, UBE2D3;CISD2, BDH2* | *SLC39A8,* ***NFKB1****, UBE2D3;CISD2, SLC9B1, BDH2* | *SLC39A8, UBE2D3, CISD2, BDH2* |
| 5 | 151064651 - 151080486 | *TNIP1* | | | | |
| 6 | 106181815 - 106339294 | *ATG5* | | | | |
| 7 | 128933913 - 129095960 | *IRF5-TNPO3* | | | | |
| 8 | 11474517 - 11544554 | *FAM167A-BLK* | | | | |
| 8 | 60638547 - 60664239 | *RAB2A-CHD7* | *ASPH, SDCBP, CHD7* | | *ASPH, SDCBP* | *ASPH, SDCBP, CHD7* |
| 11 | 554659 - 619789 | *CDHR5 -IRF7* | | | | |
| 11 | 2311894 - 2363262 | *TSPAN32,CD81-AS1* | *TSSC4* | | *TSSC4* | *TSSC4* |
| 11 | 118704617 - 118875175 | *DDX6* | *CXCR5, UPK2,* ***DDX6****, IFT46;ARCN1* | *CXCR5* | *CXCR5, UPK2,* ***DDX6*** | *CXCR5,* ***DDX6,*** *ARCN1* |
| 15 | 74739180 - 75148328 | *CSK* | ***CSK****, CLK3, ULK3, SCAMP2, MPI, FAM219B, COX5A* | ***CSK****, CLK3, ULK3, SCAMP2, MPI, FAM219B, COX5A, C15orf39* | ***CSK****, ULK3, SCAMP2, MPI, FAM219B, COX5A, C15orf39* | ***CSK****, CLK3, ULK3, SCAMP2, MPI, FAM219B, COX5A, C15orf39* |
| 16 | 85932852 - 85979945 | *IRF8* | | ***IRF8*** | ***IRF8*** | ***IRF8*** |
| 17 | 39747478 - 39933464 | *IKZF3-GSDMB* | ***IKZF3****, ERBB2, PSMD3* | *ERBB2* | ***IKZF3****, ERBB2, PSMD3* | ***IKZF3****, ERBB2, PSMD3* |
| 17 | 75193533 - 75279345 | *NUP85-GRB2* | | | | |
| 19 | 18068862 - 18093031 | *IL12RB1* | *PIK3R2, RAB3A* | *RAB3A* | *PIK3R2, RAB3A* | |

Genes classically associated with systemic sclerosis through proximity to GWAS loci are highlighted in bold.

[1]Bp in GRCh38 (hg 38) assembly

[2]Locus as defined by López-Isac et al.(9)

[3]Genes corresponding with promoter interacting regions overlapping enhancer regions and systemic sclerosis GWAS SNPs

*Bp* base pair, *Chr* chromosome, *GWAS* Genome-wide association studies, *N* number, *pCHi-C* promoter capture Hi-C, *SNP* single-nucleotide polymorphism.

**Table 2. Summary of potential targets for drug repurposing in systemic sclerosis based on pCHi-C data**

| GWAS locus | pCHi-C interacting genes | Cell type with interactions | Genes in strong PPI | Targeted drug | Disease indication[$] |
|---|---|---|---|---|---|
| *CD247* | *CREG1* | CD4+ T cells | *TUBB4B* | Colchicine | Osteoarthritis, Advanced fibrosis |
| *FLNB-DNASE1L3-PXK* | *RPP14* | CD4+ T cells, CD14+ monocytes | *KEAP1* | Dimethyl Fumarate | Psoriasis, Multiple sclerosis, Disseminated sclerosis |
| | | | *AGTR1* | Candesartan | Type 1 Diabetes |
| | | | *HSPA8* | Forigerimon | Systemic lupus erythematosus |
| *NFKB1* | *NFKB1* | CD4+ T cells | *IL12B* | Ustekinumab | Psoriasis, Crohn´s disease, Ulcerative colitis |
| | | | *IL1R1* | Anakinra | Rheumatoid arthritis |
| | | | *IL23A* | Tildrakizumab | Psoriasis |
| | | | *JAK2* | Tofacitinib | **Systemic sclerosis**, Rheumatoid arthritis, Ulcerative colitis, Interstitial lung disease, Takayasu Arteritis |
| | | | *NR3C1* | Methylprednisolone* | Rheumatoid arthritis, Crohn´s disease, Psoriatic arthritis, Ulcerative colitis, Behcet´s syndrom |
| | *UBE2D3* | CD4+ T cells, CD14+ monocytes | *KEAP1* | Dimethyl Fumarate | Psoriasis, Multiple sclerosis, Disseminated sclerosis |
| *RAB2A-CHD7* | *SDCBP* | CD4+ T cells | *IMPDH1* | Mycophenolic acid* | Systemic lupus erythematosus, Immunosuppression |
| | | | *TUBB4B* | Colchicine | Osteoarthritis, Advanced fibrosis |
| | *CHD7* | CD4+ T cells | *PPARG* | Mesalamine | Crohn's disease, Ulcerative colitis |
| *DDX6* | *CXCR5* | CD4+ T cells, CD14+ monocytes | *S1PR3* | Fingolimod | Multiple sclerosis, Disseminated sclerosis |
| *CSK* | *CSK* | CD4+ T cells, CD14+ monocytes | *FLT4* | Nintedanib | **Systemic sclerosis**, Idiopathic pulmonary fibrosis, Interstitial lung disease |
| | *COX5A* | CD4+ T cells, CD14+ monocytes | *NDUFB10* | Metformin | Type 1 Diabetes, Type 2 Diabetes |
| *IKZF3-GSDMB* | *IKZF3* | CD4+ T cells | *JAK1* | Baricitinib | Rheumatoid arthritis |
| | | | *JAK3* | Upadacitinib | Rheumatoid arthritis |
| | | | *IL2RA* | Basiliximab | Type 1 Diabetes |
| | *ERBB2* | CD4+ T cells, CD14+ monocytes | *IL6R* | Tocilizumab | **Systemic sclerosis**, Rheumatoid arthritis, Juvenile idiopathic arthritis, Giant cell arteritis |
| | | | *JAK* kinases | Tofacitinib | **Systemic sclerosis**, Rheumatoid arthritis, Ulcerative colitis, Interstitial lung disease, Takayasu Arteritis |
| *IL12RB1* | *PIK3R2* | CD4+ T cells | *ADRA1B* | Epinephrine | Crohn's disease |
| | | | *AGTR1* | Candesartan | Type 1 Diabetes |
| | | | *EDNRA* | Bosentan | **Systemic sclerosis**, Idiopathic pulmonary fibrosis, Pulmonary arteria hypertension |
| | | | *JAK1* | Baricitinib | Rheumatoid arthritis |
| | | | *JAK* kinases | Tofacitinib | **Systemic sclerosis**, Rheumatoid arthritis, Ulcerative colitis, Interstitial lung disease, Takayasu Arteritis |
| | | | *PDGFRB* | Nintedanib | **Systemic sclerosis**, Idiopathic pulmonary fibrosis, Interstitial lung disease |
| | *RAB3A* | CD4+ T cells, CD14+ monocytes | *HSPA8* | Forigerimod | Systemic lupus erythematosus |

[$]Only related immune-mediated diseases were included. All clinical trials at least in completed phase III.

*These drugs present phase III or lower clinical trials in systemic sclerosis.

*GWAS* genome-wide association studies, *pCHi-C* promoter capture Hi-C, *PPI* protein-protein interaction.

A

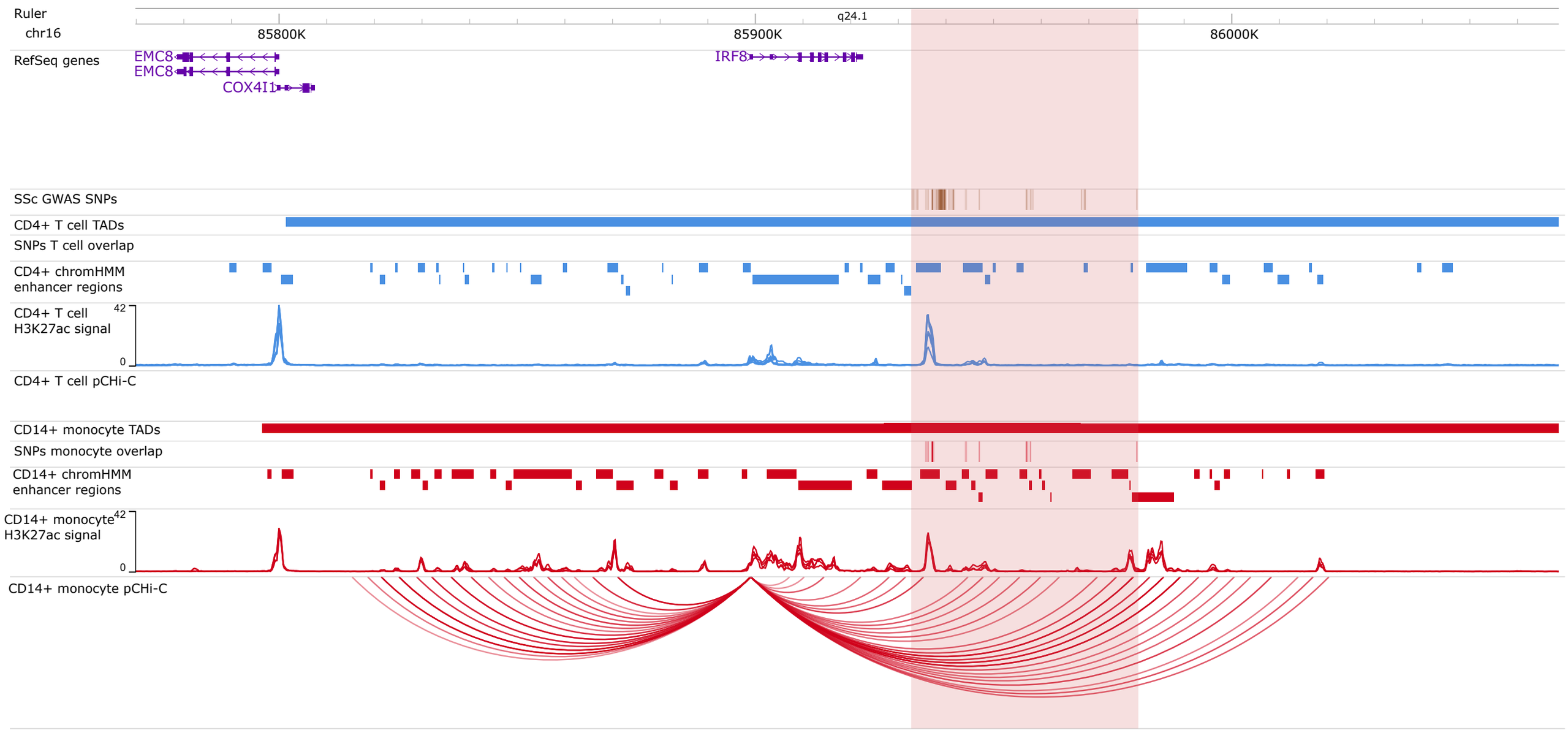
Ruler
chr16
q24.1
85800K
85900K
86000K
RefSeq genes
EMC8
EMC8
COX4I1
IRF8
SSc GWAS SNPs
CD4+ T cell TADs
SNPs T cell overlap
CD4+ chromHMM enhancer regions
CD4+ T cell H3K27ac signal
42
0
CD4+ T cell pCHi-C
CD14+ monocyte TADs
SNPs monocyte overlap
CD14+ chromHMM enhancer regions
CD14+ monocyte H3K27ac signal
42
0
CD14+ monocyte pCHi-C

B

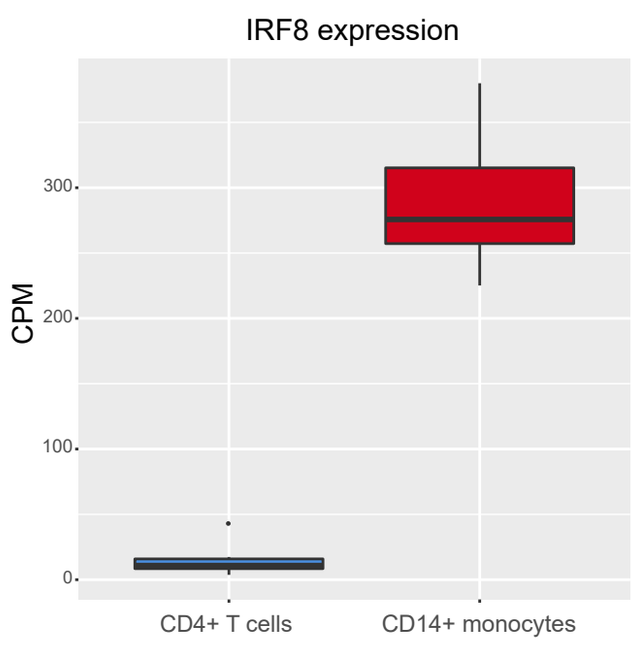
IRF8 expression
CPM
300
200
100
0
CD4+ T cells
CD14+ monocytes

C

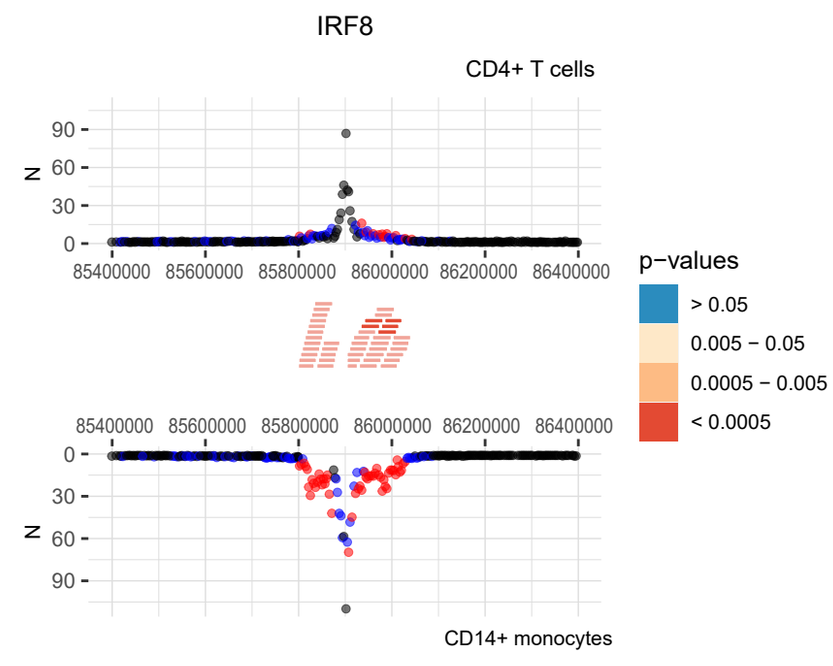
IRF8
CD4+ T cells
N
90
60
30
0
85400000
85600000
85800000
86000000
86200000
86400000
p−values
> 0.05
0.005 − 0.05
0.0005 − 0.005
< 0.0005
CD14+ monocytes

A

Ruler
chr2
K 190900K 191000K 191100K 191200K 191300K 191400K 191500K 191600K 191700K

RefSeq genes
GLS
GLS
STAT1
STAT1
STAT4
MYO1B
NABP1

SSc GWAS SNPs
CD4+ T cell TADs
SNPs T cell overlap
CD4+ chromHMM enhancer regions
CD4+ T cell H3K27ac signal
50
0
CD4+ T cell pCHi-C

CD14+ monocyte TADs
SNPs monocyte overlap
CD14+ chromHMM enhancer regions
CD14+ monocyte H3K27ac signal
50
0
CD14+ monocyte pCHi-C

B

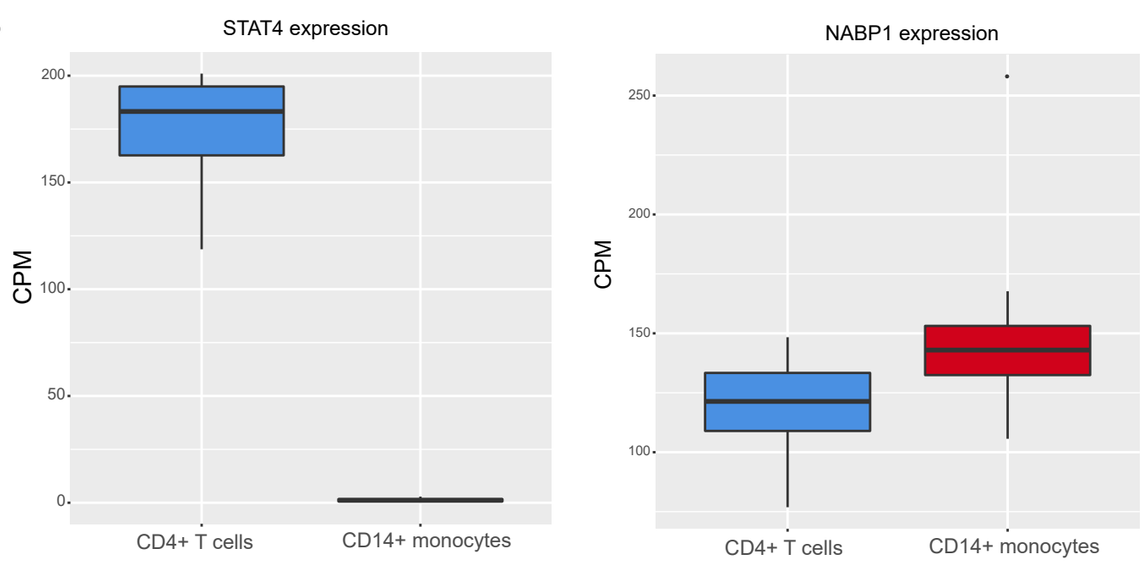


C

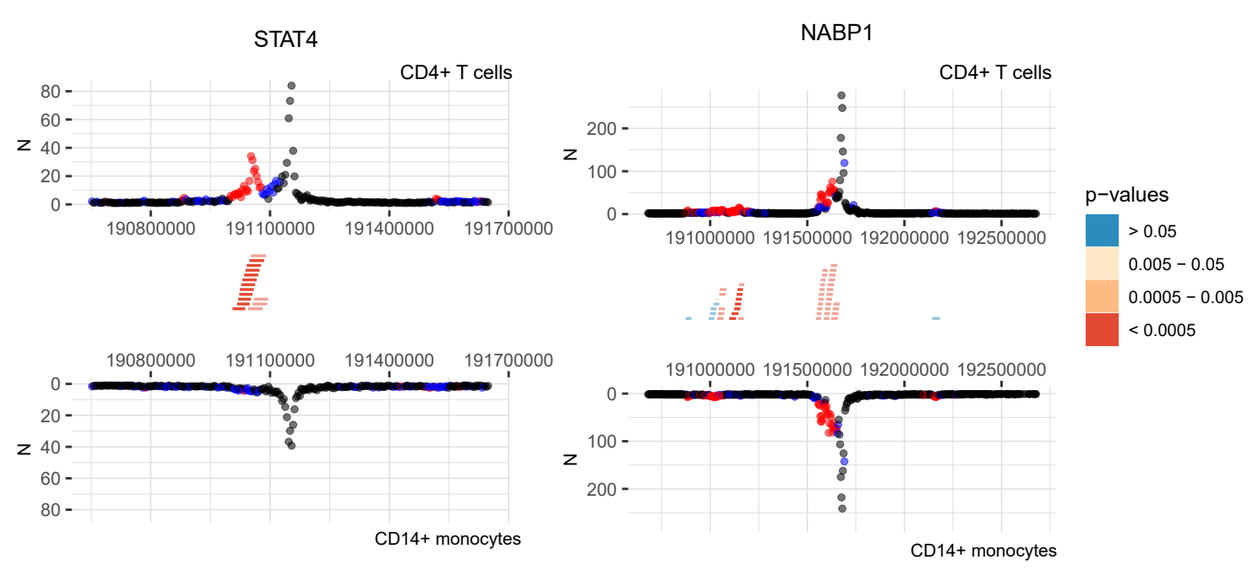

A

Ruler
chr1
000K 167100K 167200K 167300K 167400K 167500K 167600K 167700K

RefSeq genes
GPA33 MAEL DUSP27 MAEL POU2F1 POU2F1 CD247 CREG1 RCSD1 MPZL1 MPZL1

SSc GWAS SNPs
CD4+ T cell TADs
SNPs T cell overlap
CD4+ chromHMM enhancer regions
CD4+ T cell H3K27ac signal 48 0
CD4+ T cell pCHi-C

CD14+ monocyte TADs
SNPs monocyte overlap
CD14+ chromHMM enhancer regions
CD14+ monocyte H3K27ac signal 48 0
CD14+ monocyte pCHi-C

B

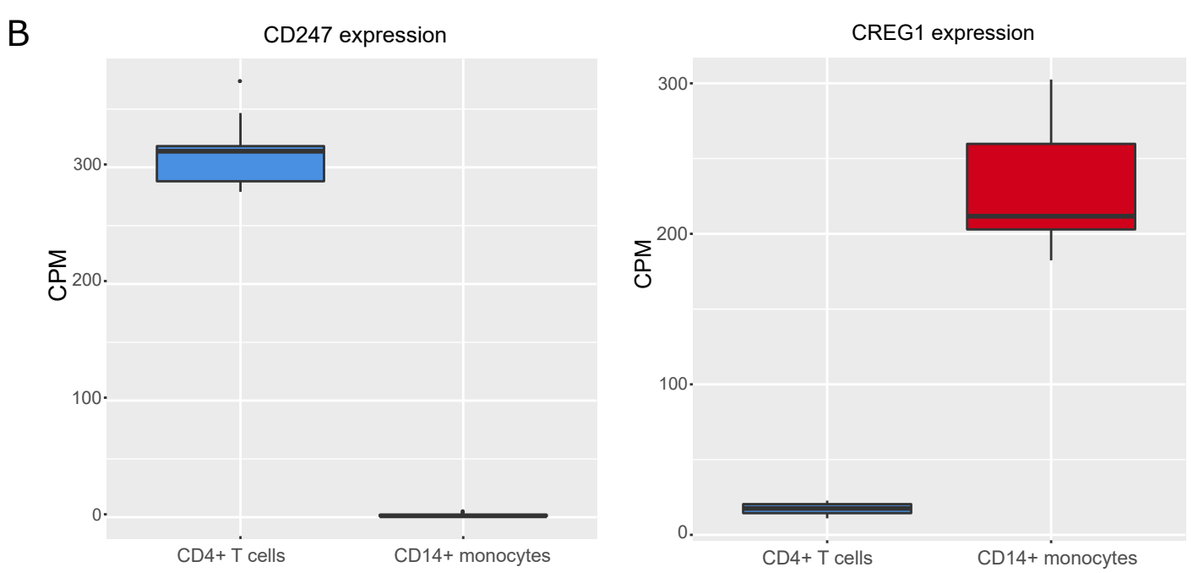


C

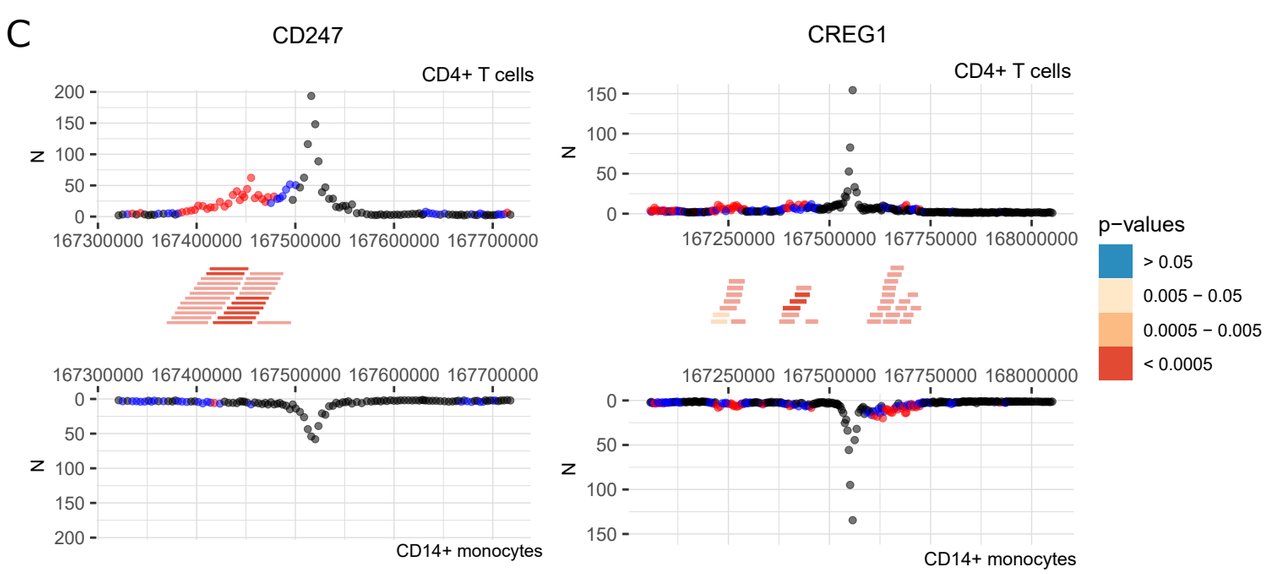

A

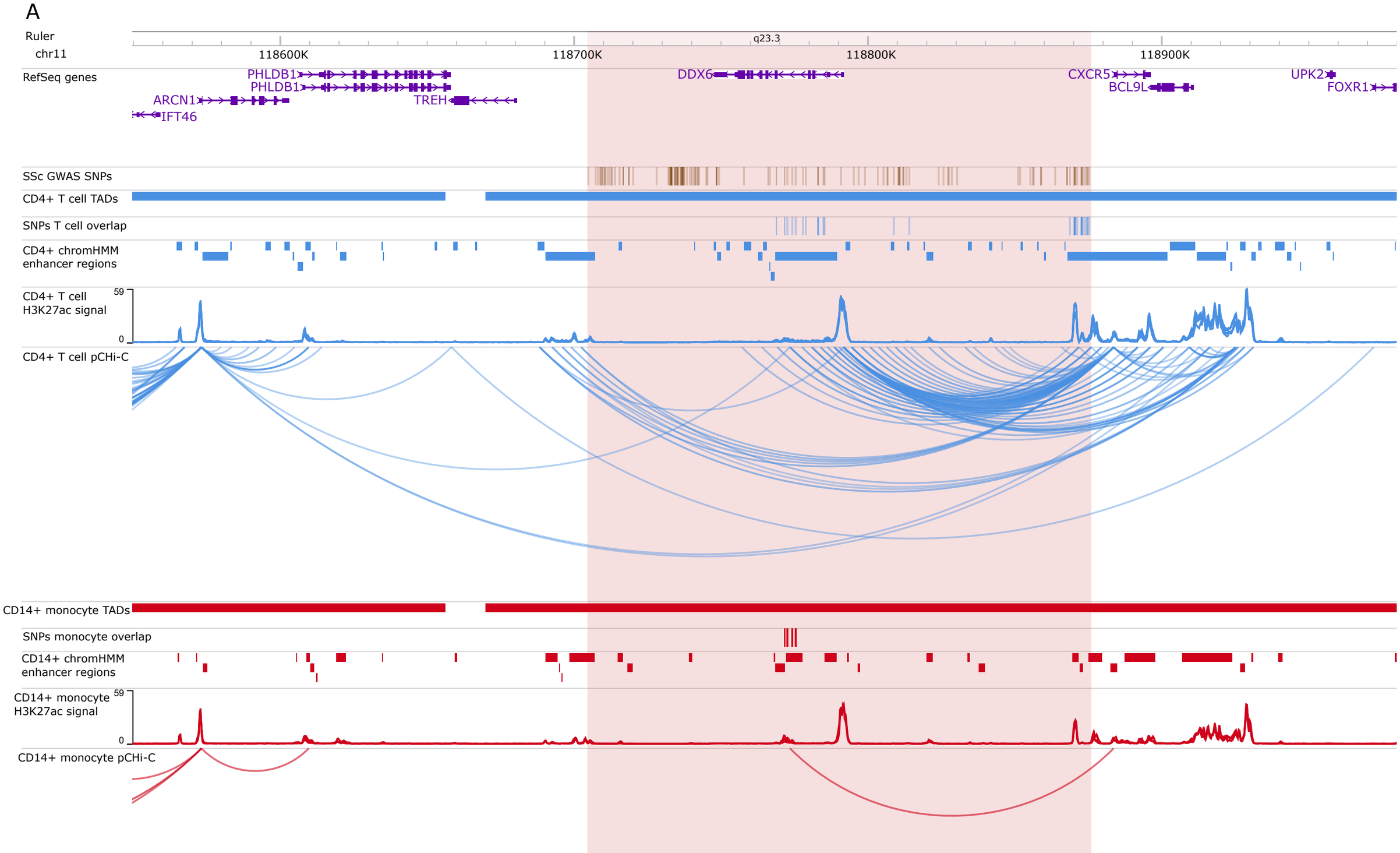
Ruler
chr11
q23.3
118600K
118700K
118800K
118900K
RefSeq genes
PHLDB1
PHLDB1
ARCN1
IFT46
TREH
DDX6
CXCR5
BCL9L
UPK2
FOXR1
SSc GWAS SNPs
CD4+ T cell TADs
SNPs T cell overlap
CD4+ chromHMM enhancer regions
CD4+ T cell H3K27ac signal
59
0
CD4+ T cell pCHi-C
CD14+ monocyte TADs
SNPs monocyte overlap
CD14+ chromHMM enhancer regions
CD14+ monocyte H3K27ac signal
59
0
CD14+ monocyte pCHi-C

B

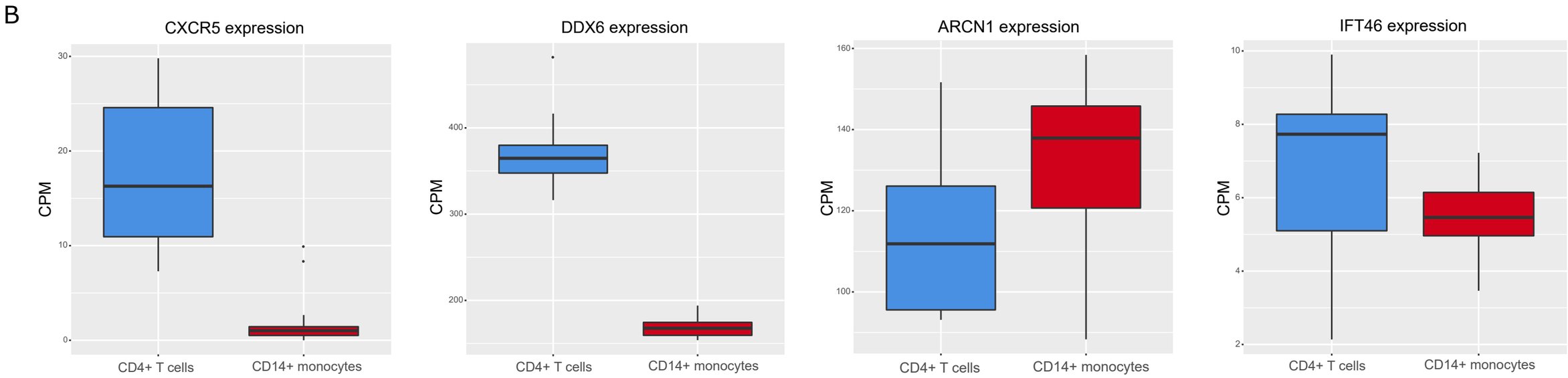
CXCR5 expression
DDX6 expression
ARCN1 expression
IFT46 expression
CPM
CD4+ T cells
CD14+ monocytes

C

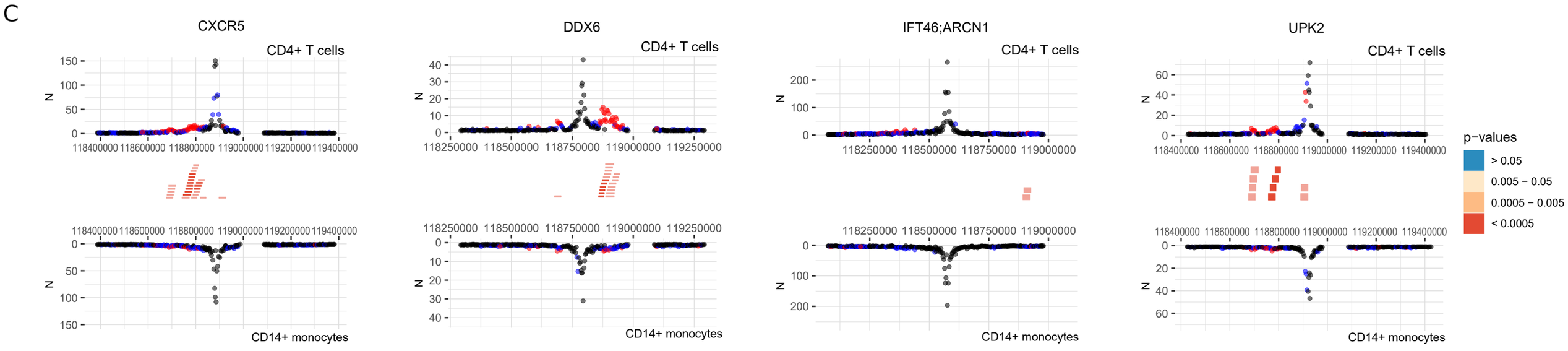
CXCR5
DDX6
IFT46;ARCN1
UPK2
CD4+ T cells
CD14+ monocytes
N
p−values
> 0.05
0.005 − 0.05
0.0005 − 0.005
< 0.0005